

# External Force Adaptive Compensator for Serial Manipulators

Albert Demian<sup>a</sup> and Alexander Klimchik<sup>b</sup>

*Center for Technologies in Robotics and Mechatronics Components, Innopolis University,  
Universitetskaya st., Innopolis, Russian Federation*

**Keywords:** Static Balancing, Force Compensation, Variable Payload, Manipulator Design.

**Abstract:** We propose a preliminary design concept for the external force compensator. An arrangement of lever-wheel arrangement with a group of springs producing counter torque to compensate for external force. The springs are fixed on adjustable pivot points to allow compensation of a range of payloads. We introduce the use of self-locking worm gears to ensure the compensator's torque is purely applied on either the wheel or the lever. We investigated the compensator design with a 2-DOF manipulator which consists of two orthogonal rotational joints. We present a design methodology to the compensator together with a selection of spring coefficients to match a certain range of payloads. Results of the simulation show complete compensation of external force is possible as compensation of certain components of the force vectors.

## 1 INTRODUCTION


Serial robotic arms are known for their various applications. The main drawback of using robot manipulators is the large mass of the links which requires using high-power motors. The majority of energy consumed during operation goes to compensate for the robot's own weight while leaving only a smaller part to manipulate payload (Kim and Song, 2014).


Studies on gravity compensation show a variety of approaches to passively compensate for the robot's weight reducing the torque required by the robot's joints (Arakelian, 2016). The traditional method is to use a counterweight (see Figure 1a) (Arakelian et al., 2000). This method allows for increasing payloads. However, it increases energy consumption as the total potential energy of the manipulator is increased due to the increased weight. Another method is to add a single-component compensator that can be spring-based or pneumatic-based as shown in Figure 1b. These elements change the non-linear dynamic behavior of the manipulator to a different behavior due to the introduction of their own non-linear behavior to the manipulator's statics and dynamics. Integrating compensators with manipulators changes stiffness properties (Klimchik and Pashkevich, 2022). An investigation of stiffness properties and identification of manipulators with spring-based compensators is

presented in (Klimchik et al., 2013), investigation of stiffness properties of manipulators with pneumatic-based compensators is presented in (Klimchik et al., 2017). Nevertheless, compensators provide support to the manipulator and enhance its stiffness properties for enhanced manipulation of payload.

Other studies introduce gravity compensation using auxiliary mechanisms with springs like the one introduced in (Gopalswamy et al., 1992). They used a parallelogram mechanism coupled with torsional springs to counter-balance gravitational torques in manipulators' joints. The advantage of using springs is that they have lightweight hence, the increase of the manipulator's total potential energy is insignificant. Studies that use springs for counter-balancing introduce various mechanisms with different types of results. An example of compensation using an auxiliary mechanism is shown in Figure 1c. Some studies show a partial reduction of gravity torques as in (Kim and Song, 2014) where they used the parallelogram mechanism as an auxiliary system to transform the vertical base axis to consequent manipulator's joints. At each joint, a spring connects between the link and the vertical reference frame allowing the compensation of the major part of the joint's torque. partial compensation of gravity torques for different types of manipulators was considered by (Morita et al., 2003), (Agrawal and Fattah, 2004), (Kim et al., 2016) and (Chung et al., 2016) where planar and a special cases were investigated.

The design of compensator for multi-DoF manip-

<sup>a</sup>  <https://orcid.org/0000-0003-1318-9220>

<sup>b</sup>  <https://orcid.org/0000-0002-2244-1849>

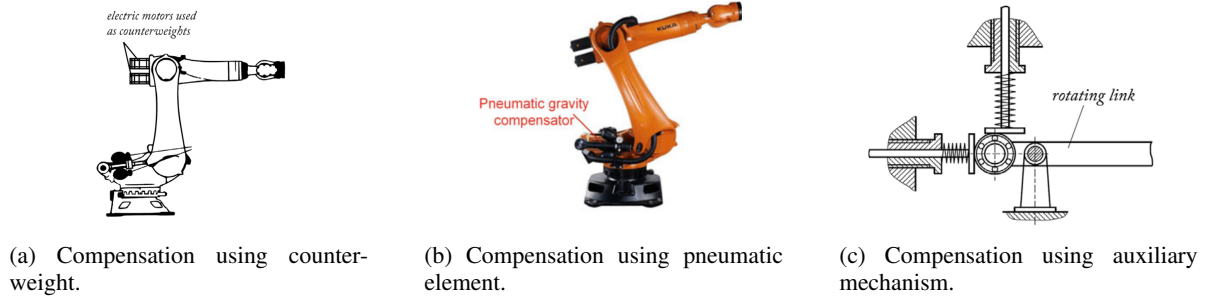


Figure 1: Different methods for counter-balancing.

ulators is complex and increases in complexity for a larger number of degrees of freedom. Another factor that affects complexity is the level of compensation as partial compensation of gravity torques is less complex than complete compensation. Moreover, designing a compensator for a planar case is less complex than for a spacial case. (Cho and Kang, 2014) proposed an analytical approach based on the analysis of the eigenvalues of the potential energy of articulated manipulators. The advantage of this approach is that it shows the decoupling of torque terms and provides a systematic approach for determining the number of springs needed and their locations. Similarly (Cho et al., 2012), (Kim and Cho, 2017), (Lin et al., 2010) and (Chung et al., 2016) considered the complexity of the spacial for complete compensation of gravity torques. While some studies considered planar cases as in (Lin et al., 2012) and (Jhuang et al., 2018). Some studies considered reducing the complexity by introducing different components as cams (Koser, 2009). Other studies went beyond service manipulators and considered different systems like rehabilitation devices as in (Nakayama et al., 2009).

In this paper, we are considering a preliminary concept of an adaptive compensator in which a combination of linear springs is integrated. The adaptation appears in the form of adjustment of springs fixation points in order to produce various values of counter-torque for the same robot configuration. This aims to compensate payload and adapt to the changes in the payload. The concept depends on coupling robot joints with a combination of springs producing a sum of torque to counter the payload torque. This allows complete compensation for the constant payload around the robot's whole workspace while being able to re-adjust components' stiffness to match different payloads. A 2-DoF spacial manipulator is mounted with the proposed compensator. We considered the arrangement of the mechanical connections however, we did not present calculations of transmission ratios. The system is tested in simulation and the results together with design recommendations are presented.

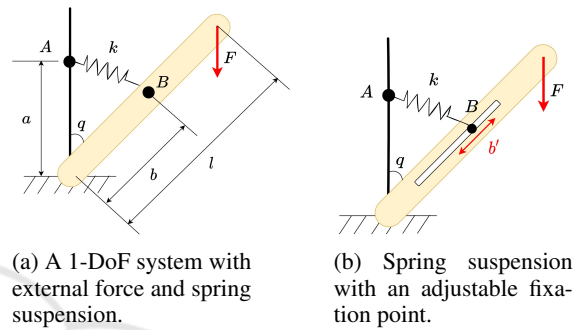


Figure 2: Compensation of a single-component force with 1-DoF system.

## 2 STATIC MODELING FOR A SINGLE-COMPONENT FORCE COMPENSATOR

A single-component force compensator is addressed in this section. The goal is to show a method to compensate a force component using a single spring by adjusting one of its fixation points. Figure 2a shows a 1-DoF system with one link of length  $l$  and rotated with angle  $q$ . The mass of the link is not considered. A spring with stiffness coefficient  $k$  is connected at point  $A$  at a vertical distance  $a$  from the ground and at point  $B$  at distance  $b$  along the link. An external force  $F$  is applied on the tip of the link pointing downwards making the force vector  $F = [0, 0, -f_z]^T$  and the tip position as follows.

$$\vec{L} = [l \sin(q) \quad 0 \quad l \cos(q)]^T \quad (1)$$

where  $\vec{L}$  is the position vector pointing from the center of rotation to the tip of the link.

It is possible to calculate the torque due to external force using cross product.

$$\tau = \vec{L} \times F = [0 \quad -f_z l \sin(q) \quad 0]^T \quad (2)$$

where  $\tau$  is the torque due to external force around the center of rotation.

A spring with proper stiffness coefficient can produce counter torque that eliminates the effect of the force and makes the sum of torques around the joint equals to zero at any angle  $q$ .

$$F_s = \vec{BA} k \tag{3}$$

where  $k$  is the spring's stiffness coefficient,  $\vec{BA}$  is the distance vector pointing from point  $B$  to point  $A$  representing the extended length of the spring and  $F_s$  is the force produced by the spring.

$$\tau_s = \vec{B} \times F_s = [0 \quad a b k \sin(q) \quad 0]^T \tag{4}$$

where  $\tau_s$  is the torque produced by the spring around the center of rotation.

As the system should be in equilibrium, the sum of torques should be zero  $\tau + \tau_s = 0$ .

$$a b k \sin(q) = f_z l \sin(q) \tag{5}$$

And accordingly we can choose the spring coefficient  $k$ .

$$k = \frac{f_z l}{a b} \tag{6}$$

Figure 2b shows an adjustable pivot point where only one of the spring's ends is fixed. By adjusting the distance  $b'$ , we can achieve compensation to a range of values of applied force.

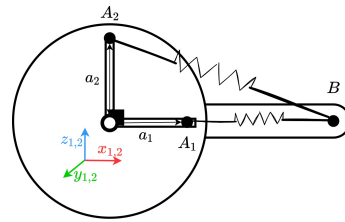
$$b' = f_z \frac{l}{a k} \tag{7}$$

This implies a linear relation between the distance  $b'$  and the applied force. This means that the linear variation of the distance  $b'$  can correspond to a value range of force that can be compensated.

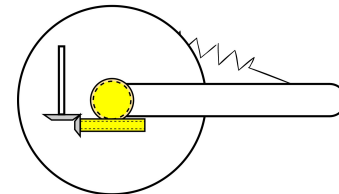
### 3 STATIC MODELING FOR A TWO-COMPONENT FORCE COMPENSATOR

For systems with multi-DoF, the torque applied on a single joint due to external force depends on the whole configuration of the manipulator. This section aims to show a method using two springs to produce a counter-torque that depends on two configuration angles  $\theta_1$  and  $\theta_2$ . Figure 3a shows lever-wheel arrangement. The lever and the wheel rotate around the same center with angles  $\theta_1$  and  $\theta_2$ , respectively. Two points  $A_1$  and  $A_2$  are fixed at some distance  $a_1$  and  $a_2$  from the center of the wheel and set apart with a 90 shift. Point  $B$  is fixed at distance  $b$  along the lever. Two springs with coefficients  $[k_1, k_2]$  connect point  $B$  with both points  $A_1$  and  $A_2$ , respectively.

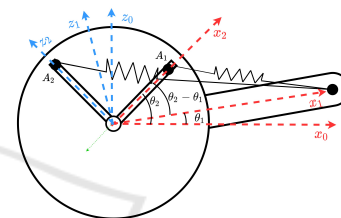
Taking the lever rotation of the value  $\theta_1$  while the rotation of the wheel of  $\theta_2$ . If the wheel and the lever



(a) Geometric representation of lever-wheel mechanism with 2-DoF compensator.



(b) Geometrical representation of worm gear meshing on the back side of the lever-wheel mechanism.



(c) A show case where the lever rotates with angle  $\theta_1$  while the wheel rotates with angle  $\theta_2$ .

Figure 3: The concept of using the lever-wheel arrangement.

rotate in the same direction, a value of  $(\theta_1 - \theta_2)$  can be realized. While if they rotate in opposite directions, a value  $(\theta_1 + \theta_2)$  can be realized, taking the counter-clockwise direction as the positive direction. Figure 3c presents realization of  $\theta_1 - \theta_2$ . Taking the lever's reference frame where the x-axis points along the lever, makes the position vector of points  $A_1, A_2$  and  $B$  as follows:

$$B = [b, 0, 0]^T$$

$$A_1 = a_1 [\cos(\theta_1 - \theta_2) \quad 0 \quad \sin(\theta_1 - \theta_2)]^T \tag{8}$$

$$A_2 = a_2 [-\sin(\theta_1 - \theta_2) \quad 0 \quad \cos(\theta_1 - \theta_2)]^T$$

The torque generated by the spring between points  $A_1$  and  $B$  can be formulated as follows:

$$\tau_{a_1} = k_1 \cdot A_1 \times (B - A_1) \tag{9}$$

where  $k_1$  is the stiffness coefficient of the spring connecting between points  $A_1$  and  $B$  and  $\tau_{a_1}$  is the torque produced by this spring.

$$\tau_{a_1,y} = -k_1 a_1 b \sin(q_1 - q_2) \tag{10}$$

where  $\tau_{a_1,y}$  is the y-component of  $\tau_{a_1}$  as the x and z components equal to zero.

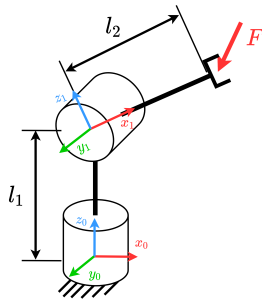


Figure 4: 2DoF manipulator.

Similarly, for the spring between points  $A_2$  and  $B$ :

$$\tau_{a_2} = k_2 \cdot A_2 \times (B - A_2) \quad (11)$$

which makes the y-component  $\tau_{a_1,y}$  as follows.

$$\tau_{a_2,y} = -k_2 a_2 b \cos(q_1 - q_2) \quad (12)$$

Making the sum of torques  $\tau_{sum}$  around the center of rotation as follows:

$$\begin{aligned} \tau_{sum} &= \tau_{a_1,y} + \tau_{a_2,y} \\ &= -k_1 a_1 b \sin(q_1 - q_2) - k_2 a_2 b \cos(q_1 - q_2) \end{aligned} \quad (13)$$

Using a self-locking worm gear ensures that the torque is applied on the wheel and prevents the lever from getting affected by this torque. Figure 3b shows that the lever is coupled with a worm gear. We can realize different values for  $\tau_{sum}$  by making distances  $a_1$  and  $a_2$  to be adjustable as illustrated for the case in Figure 2.

## 4 STATIC MODELING FOR A FORCE COMPENSATOR FOR A 2-DoF MANIPULATOR

This section presents the use of the system proposed in Section 3 to compensate a 3D external force acting on the end effector of a 2-DoF manipulator shown in Figure 4. It has two orthogonal rotational joints rotate with joint coordinates  $q_1$  and  $q_2$  with links' length  $l_1$  and  $l_2$ . An arbitrary force  $F = [f_x, f_y, f_z]^T$  is applied on the tip of the second link. The goal is to compensate torque of the manipulator's joints using the system presented in Figure 3. we can calculate the manipulator's tip pose and the manipulator Jacobian taking and arbitrary configuration  $Q = [q_1, q_2]^T$  as follows:

$$X = \begin{bmatrix} l_2 \sin(q_2) \cos(q_1) \\ l_2 \sin(q_2) \sin(q_1) \\ l_1 + l_2 \cos(q_2) \end{bmatrix} \quad (14)$$

where  $X$  is a 3D position vector representing position of the end effector.

Then we can derive the manipulator Jacobian by calculating the partial derivative of the vector  $X$  with respect to joint coordinates  $\partial X / \partial q_i$

$$J = \begin{bmatrix} -l_2 \sin(q_1) \sin(q_2) & l_2 \cos(q_1) \cos(q_2) \\ l_2 \sin(q_2) \cos(q_1) & l_2 \sin(q_1) \cos(q_2) \\ 0 & -l_2 \sin(q_2) \end{bmatrix} \quad (15)$$

where  $J$  is the manipulator's Jacobian.

The Jacobian matrix is used to map the external force to joints' torques by taking its transpose.

$$\tau = J^T F \quad (16)$$

where  $\tau$  is vector of joint torques  $[\tau_1, \tau_2]^T$  and  $F$  is the applied external force vector.

This makes torque of the joints as follows.

$$\tau_1 = -f_x l_2 \sin(q_1) \sin(q_2) + f_y l_2 \cos(q_1) \sin(q_2) \quad (17)$$

where  $\tau_1$  is the torque in the first joint.

$$\begin{aligned} \tau_2 &= f_x l_2 \cos(q_1) \cos(q_2) \\ &\quad + f_y l_2 \sin(q_1) \cos(q_2) - f_z l_2 \sin(q_2) \end{aligned} \quad (18)$$

where  $\tau_2$  is the torque in the second joint.

We can expand the torque formulas using the trigonometric identities switching multiplication into addition as follows:

$$\begin{aligned} \tau_1 &= \frac{1}{2} f_x l_2 \cos(q_1 + q_2) - \frac{1}{2} f_x l_2 \cos(q_1 - q_2) \\ &\quad + \frac{1}{2} f_y l_2 \sin(q_1 + q_2) - \frac{1}{2} f_y l_2 \sin(q_1 - q_2) \end{aligned} \quad (19)$$

and similarly for  $\tau_2$

$$\begin{aligned} \tau_2 &= \frac{1}{2} f_x l_2 \cos(q_1 + q_2) + \frac{1}{2} f_x l_2 \cos(q_1 - q_2) \\ &\quad + \frac{1}{2} f_y l_2 \sin(q_1 + q_2) + \frac{1}{2} f_y l_2 \sin(q_1 - q_2) \\ &\quad - f_z l_2 \sin(q_2) \end{aligned} \quad (20)$$

This expansion of torque expressions shows the similarity between those expressions and the one derived from the system in Section 3. This means that it is possible to design a combination of the system in Figure 3a to compensate for the external force acting on the manipulator.

### 4.1 Compensator Design for the First Joint

Using the system in Figure 3, we can compensate for the torque applied to the joint. The system in Figure 3c compensates for terms with angle difference

$q_1 - q_2$ . A second system where the level rotates in the reverse direction can be used to compensate for terms with angle sum  $q_1 + q_2$ . Considering the wheels rotate with angle  $q_1$  and one lever rotates with angle  $q_2$  and  $-q_2$ , respectively. This will allow realizing all the four terms in Eqn. (19). Each system has a point B and 2 points A. This makes the compensator for the first joint has two points  $B_1$  and  $B_2$  and 4 points  $A_1, A_2, A_3$  and  $A_4$ . Due to mechanical constraints, points  $A_1, A_2, A_3$  and  $A_4$  will be fixed to the ground while points  $B_1$  and  $B_2$  are can rotate with angles  $q_1 - q_2$  and  $q_1 + q_2$ , respectively. When the second joint rotates with angle  $q_2$ , the lever angles can be adjusted by values  $q_2$  and  $-q_2$ , respectively. The counter-torque will compensate for the torque of the first joint as the worm gear will eliminate the reaction on the second joint. By realizing this system, the value of the counter-torque will be as follows:

$$\tau_{c,1} = k_1 a_1 b_1 \cos(q_1 - q_2) + k_2 a_2 b_1 \sin(q_1 - q_2) - k_3 a_3 b_2 \cos(q_1 + q_2) - k_4 a_4 b_2 \sin(q_1 + q_2) \quad (21)$$

By comparing eqs. (19) and (21), we can find equivalent terms where nonlinear terms can be eliminated and we can realize sum of torques  $\tau_1 + \tau_{c,1} = 0$ . We can select spring constants as follows:

$$\frac{f_x l_2 \cos(q_1 - q_2)}{2} = k_1 a_1 b_1 \cos(q_1 - q_2) \quad (22)$$

which makes  $k_1$  as follows:

$$k_1 = \frac{f_x l_2}{2 a_1 b_1} \quad (23)$$

similarly for the  $k_2, k_3$  and  $k_4$ , we get the following expressions:

$$k_2 = \frac{f_y l_2}{2 a_2 b_1} \quad k_3 = \frac{f_x l_2}{2 a_3 b_2} \quad k_4 = \frac{f_y l_2}{2 a_4 b_2} \quad (24)$$

Here, we managed to select stiffness coefficients of the springs that would compensate the torque on the first joint at any configuration.

## 4.2 Compensator for the Second Joint

Performing the same procedure as for the first joint, we can choose the design parameters for the second joint. Here, there will be an extra component added to compensate for the 5<sup>th</sup> term  $-f_z l_2 \sin(q_2)$  in Eqn. (20) which is similar to the system in Figure 2b. This makes the compensator for the second joint contain 5 springs, 5 points  $A_i$ , and 3 points  $B_j$ .

$$\tau_{c,2} = -k_5 a_5 b_3 \cos(q_1 + q_2) - k_6 a_6 b_3 \sin(q_1 + q_2) - k_7 a_7 b_4 \cos(q_1 - q_2) - k_8 a_8 b_4 \sin(q_1 - q_2) + k_9 a_9 b_5 \sin(q_2) \quad (25)$$

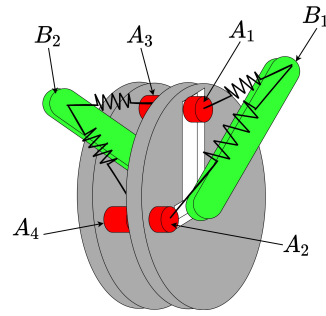


Figure 5: Model of adaptive force compensator for the first joint; mechanical coupling of  $A_1$  with  $A_3$  and  $A_2$  with  $A_4$ .

We can choose spring constant using the same procedure as for the first compensator.

$$k_5 = \frac{f_x l_2}{2 a_5 b_3} \quad k_6 = \frac{f_y l_2}{2 a_6 b_3} \quad k_7 = \frac{f_x l_2}{2 a_7 b_4} \quad (26)$$

$$k_8 = \frac{f_y l_2}{2 a_8 b_4} \quad k_9 = \frac{f_z l_2}{a_9 b_5}$$

At this point, a compensation scheme for the whole manipulator is realized based on the presented equations. Although the number of parameters to be adjusted to achieve adaptation is big, further reduction is possible due to mechanical constraints that can be imposed.

## 4.3 Parameters Reduction

To realize this derivation into mechanical implementation of these parameters means we will need to add 9 adapting actuators to adjust points  $[A_1, A_2, \dots, A_9]$ . However, we can see similarities that will allow further reduction of the adaptation parameters. As we can select distances  $a_i$  as design parameters, we are allowed to assume equality relationships between corresponding points. For example, eqs. (23) and (24) show that if we select  $k_1 = k_3$ , we can mechanically couple points  $A_1$  and  $A_3$ . hence, distances  $a_1$  is equal to  $a_3$  and by turn distance  $b_1$  is equal to  $b_2$ .

$$\frac{f_x l_2}{2 a_1 b_1} = \frac{f_x l_2}{2 a_3 b_2} \quad (27)$$

Applying the same concept to  $k_2$  and  $k_4$ , makes distance  $a_2 = a_4$ . Figure 5 shows a scheme of compensator realization for the first joint.

As for the second joint, we can do the same for eqn. (26). This allows mechanical coupling of points  $a_5$  with  $a_7$  and  $a_6$  with  $a_8$  provided that distance  $b_3 = b_4$ .

Applying these constraints, counter torque terms  $\tau_{c,1}$  and  $\tau_{c,2}$  can be reduced as follows:

$$\tau_{c,1} = k_1 a_1 b_1 (\cos(q_1 - q_2) - \cos(q_1 + q_2)) + k_3 a_3 b_1 (\sin(q_1 - q_2) - \sin(q_1 + q_2)) \quad (28)$$

$$\begin{aligned} \tau_{c,2} = & k_5 a_5 b_3 (-\cos(q_1 - q_2) - \cos(q_1 + q_2)) \\ & + k_6 a_6 b_3 (-\sin(q_1 - q_2) - \sin(q_1 + q_2)) \\ & + k_9 a_9 b_5 \sin(q_2) \quad (29) \end{aligned}$$

Each of counter torque EQs. (21) and (25) can be realized as an independent system mounted on the corresponding actuator's shaft. The wheel mounting points  $A_i$  are rigidly coupled with the actuator's shaft while the lever mounting point  $b_j$  is connected with the other actuator to realize the value of  $q$  or  $-q$ . Figure 6 shows a scheme of how the model can be realized.

#### 4.4 Adaptation to Change in External Force

The proposed derivation of counter-torque and design realization shows a method to achieve static balancing to some arbitrary external force. However, in reality, it is more realistic to have a counterbalancing mechanism that can adapt to a range of forces. We propose to make distances  $a_i$  variable so it allows the counter-torque mechanisms to produce a range of torques that can statically compensate for a value range of external force. This became possible as this approach introduces decoupling of torque components that can be realized into simple mechanical components which consist of simple mechanisms as shown in Figure 3a. Depending on the scheme introduced in Figure 5, it is possible to mount linear actuators to adjust distances  $a_i$ . In the case of the first joint, only two linear actuators are needed to adjust counter torque. As for the second joint, three linear actuators are needed. we can rewrite EQs. (19) and (20) to match EQs. (28) and (29), respectively.

$$\begin{aligned} \tau_1 = & \frac{1}{2} f_x l_2 (\cos(q_1 + q_2) - \cos(q_1 - q_2)) \\ & + \frac{1}{2} f_y l_2 (\sin(q_1 + q_2) - \sin(q_1 - q_2)) \quad (30) \end{aligned}$$

$$\begin{aligned} \tau_2 = & \frac{1}{2} f_x l_2 (\cos(q_1 + q_2) + \cos(q_1 - q_2)) \\ & + \frac{1}{2} f_y l_2 (\sin(q_1 + q_2) + \sin(q_1 - q_2)) \\ & - f_z l_2 \sin(q_2) \quad (31) \end{aligned}$$

By examining corresponding terms in torque and counter-torque equations, we can find that each adaptive parameter corresponds to the force's components. For example, taking correspondence of the first term of both EQs. (30) and (28) we can find that distance  $a_1$  affects the counter-torque part that corresponds only

to the force component  $f_x$ . Hence, we can deduce the value of distance  $a_1$  only based on the value of  $f_x$ .

$$a_1 = f_x \frac{l_2}{2 k_1 b_1} \quad (32)$$

Similarly, for other force components, we can find that each component has a corresponding adjustable parameter in each joint. For change in the value  $f_x$ , it is enough to adjust distances  $a_1$  and  $a_5$ . Also, for change in the value of  $f_y$ , distances  $a_3$  and  $a_6$  need to be adjusted. While for changes in  $f_z$ , only distance  $a_9$  needs to be adjusted.

The choice of spring constants  $k_i$  can be done provided the design requirements. The range of payload is a design requirement that is necessary to meet. To achieve this, we need to decide on the range of payload force  $[f_{min}, f_{max}]$  and on the range of distance  $a$   $[a_{min}, a_{max}]$ . Then we can choose the proper value of the spring constant to achieve this ratio as follows.

$$k_i = \frac{f_{(x,y,z),max} - f_{(x,y,z),min}}{a_{j,max} - a_{j,min}} \frac{2 b_k}{l_2} \quad (33)$$

where  $f_{(x,y,z)}$  is either  $x, y$  or  $z$  component of the applied force.

This implies that we can choose spring coefficients to match a desired range of payload. This means that it is possible to change the range of force compensation by only changing the spring coefficients for the same geometric model of the manipulator.

## 5 DISCUSSION

The proposed system presents a preliminary concept to completely compensate joints' torque due to an external force. As a manipulator is a multi-body mechanism, the external force applied on the end effector introduces non-linear torque on the manipulator's joints. This approach depends on the decomposition of non-linear terms and introduces equivalent mechanical components with linear springs to counter this non-linear torque. By coupling these mechanical components with the manipulator's joints, they can apply a sum of torques that is equivalent to the applied torque to achieve static balancing.

It is useful to select design parameters according to a range of payloads. As eqn. 33 shows that the ratio  $f/a$  is constant and allows an easy choice of the value of the corresponding spring constant. The choice of the other parameters is mainly geometrical and bound to the dimensions of the manipulator and available space.

The use of self-locking worm gears is crucial to realizing this concept. The worm gear ensures the

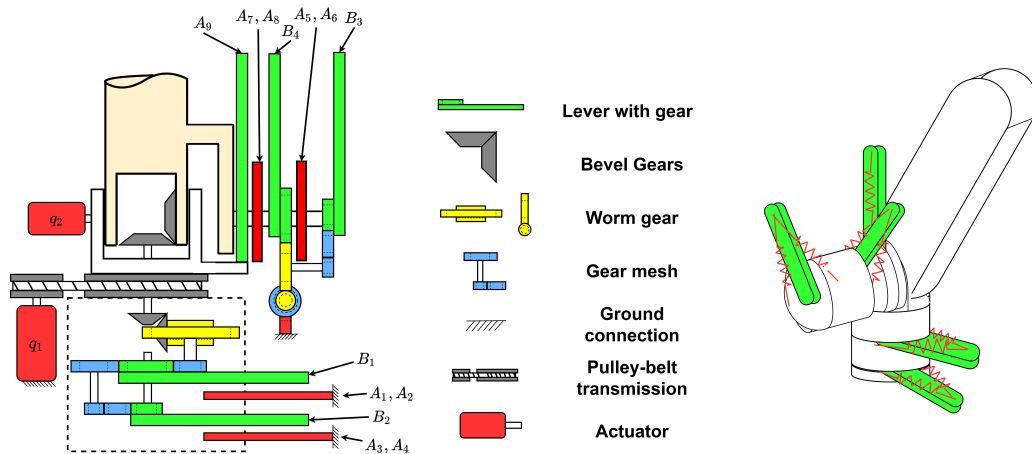


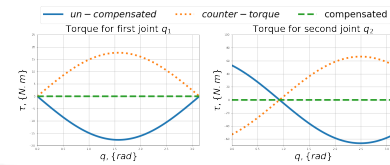
Figure 6: A schematic representation of system assembly.

pure application of the counter-balancing torque on the intended joint and blocks any reverse torque from displacing other joints. It acts as a one-way gate to both motion and torque. This allows mechanical position feedback from other joints to the compensator of a certain joint while these joints will not be affected by the counter-balancing torque produced by this certain compensator. Other mechanical components are introduced to realize correct motion ratios.

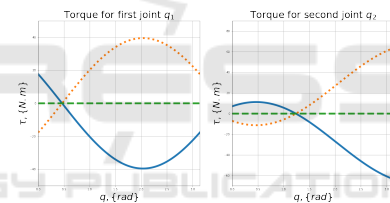
## 6 RESULTS

Two main scenarios were tested in simulation. The first case is when  $q_1$  was given a constant arbitrary value  $\pi/4$  while  $q_2$  is spanning between  $[0, \pi]$ . In the second case, it is the reverse of the first case. Link length were assigned the values  $l_1 = l_2 = 500mm$ . The value of distances  $[b_1, \dots, b_5]$  are assigned a constant value of  $250 mm$ . Span distance of  $[a_1, \dots, a_9]$  is assigned to be  $[0 : 100] mm$ . An external force of value  $F = [100, 50, 80]^T (N)$  is applied on the tip of the second link. Values of spring constants  $k_i$  are calculated using eqs. (23),(24) and (26). Simulation results show that we can achieve complete compensation of external force in any configuration around the work space. Figure 7 shows the simulation's results.

The selection of spring constants can be adjusted provided the range of external force acting on the end effector. It is more practical to select the design parameters of a robotic system according to the intended payload for this system. Selecting the range of payload and range of length  $a_j$  as design parameters can help with choosing the proper value of the spring constant. Figure 8 shows different ranges of force components that the system can compensate for with different values of  $k_i$  provided the range of distance  $a_j$ .



(a)  $q_1 = \pi/4$  and  $q_2$  spans  $[0 : \pi]$ .



(b)  $q_2 = \pi/4$  and  $q_1$  spans  $[0 : \pi]$ .

Figure 7: Torque of the 2-DoF manipulator with the proposed force compensator.

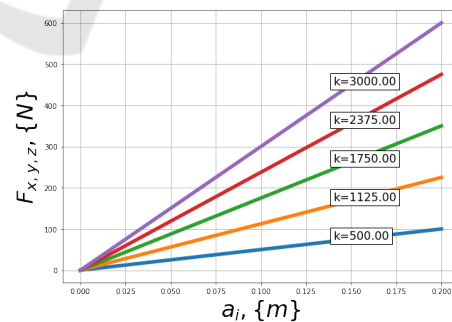


Figure 8: Range of force compensation for different values of  $k$  with certain range of distance  $a$ .

## 7 CONCLUSION

This paper proposes a preliminary concept for an adaptive external force compensator in which a com-

bination of springs is integrated. Springs' fixation points can be adjusted to produce a counter-torque that can statically balance a range of applied external forces. The design of this compensator shows that torque due to payload can be decoupled and compensated with a combination of linear springs. Variation of payload can be compensated by adjusting the distance of one of the springs' fixation points. The ratio between the range of the payload and the distance that can be spanned by the fixation point can determine the value of the spring coefficient. The paper presents the use of the compensator with a 2-DoF manipulator. The simulation shows that a complete compensation of constant payload can be achieved around the whole workspace. The adaptation feature allows complete compensation in case the payload has changed. The design of this system is very complex yet, possible. This system can be very useful in repetitive tasks with constant payload while having the advantage of readjusting for different tasks with different payloads. The advantage of this system is that it reduces energy consumed to support payload as the robot's actuators need only to support dynamic torques.

In the future, it will be necessary to use this compensator with manipulators with more than 2-DoF and to test it on real hardware.

## ACKNOWLEDGEMENTS

This work was supported by Russian Scientific Foundation (Project number 22-41-02006).

## REFERENCES

- Agrawal, S. K. and Fattah, A. (2004). Gravity-balancing of spatial robotic manipulators. volume 39, pages 1331–1344. Elsevier Ltd.
- Arakelian, V. (2016). Gravity compensation in robotics. *Advanced Robotics*, 30:79–96.
- Arakelian, V., Dahan, M., and Smith, M. (2000). A historical review of the evolution of the theory on balancing of mechanisms. In Ceccarelli, M., editor, *International Symposium on History of Machines and Mechanisms Proceedings HMM 2000*, pages 291–300, Dordrecht. Springer Netherlands.
- Cho, C. and Kang, S. (2014). Design of a static balancing mechanism for a serial manipulator with an unconstrained joint space using one-dof gravity compensators. *IEEE Transactions on Robotics*, 30:421–431.
- Cho, C., Lee, W., Lee, J., and Kang, S. (2012). A 2-dof gravity compensator with bevel gears. *Journal of Mechanical Science and Technology*, 26:2913–2919.
- Chung, D. G., Hwang, M., Won, J., and Kwon, D.-S. (2016). Gravity compensation mechanism for roll-pitch rotation of a robotic arm. In *2016 IEEE/RSJ International Conference on Intelligent Robots and Systems (IROS)*, pages 338–343.
- Gopalswamy, A., Gupta, P., and Vidyasagar, M. (1992). A new parallelogram linkage configuration for gravity compensation using torsional springs. In *Proceedings 1992 IEEE International Conference on Robotics and Automation*, pages 664–665. IEEE Computer Society.
- Jhuang, C. S., Kao, Y. Y., and Chen, D. Z. (2018). Design of one dof closed-loop statically balanced planar linkage with link-collinear spring arrangement. *Mechanism and Machine Theory*, 130:301–312.
- Kim, H. S., Min, J. K., and Song, J. B. (2016). Multiple-degree-of-freedom counterbalance robot arm based on slider-crank mechanism and bevel gear units. *IEEE Transactions on Robotics*, 32:230–235.
- Kim, H.-S. and Song, J.-B. (2014). Multi-dof counterbalance mechanism for a service robot arm. *IEEE/ASME Transactions on Mechatronics*, 19:1756–1763.
- Kim, S. H. and Cho, C. H. (2017). Static balancer of a 4-dof manipulator with multi-dof gravity compensators. *Journal of Mechanical Science and Technology*, 31:4875–4885.
- Klimchik, A. and Pashkevich, A. (2022). *Stiffness Modeling for Gravity Compensators*, pages 27–71. Springer International Publishing, Cham.
- Klimchik, A., Pashkevich, A., Caro, S., and Furet, B. (2017). Calibration of industrial robots with pneumatic gravity compensators. In *2017 IEEE International Conference on Advanced Intelligent Mechatronics (AIM)*, pages 285–290. IEEE.
- Klimchik, A., Wu, Y., Dumas, C., Caro, S., Furet, B., and Pashkevich, A. (2013). Identification of geometrical and elastostatic parameters of heavy industrial robots. In *2013 IEEE International Conference on Robotics and Automation*, pages 3707–3714. IEEE.
- Koser, K. (2009). A cam mechanism for gravity-balancing. *Mechanics Research Communications*, 36:523–530.
- Lin, P. Y., Shieh, W. B., and Chen, D. Z. (2010). Design of a gravity-balanced general spatial serial-type manipulator. *Journal of Mechanisms and Robotics*, 2.
- Lin, P. Y., Shieh, W. B., and Chen, D. Z. (2012). Design of statically balanced planar articulated manipulators with spring suspension.
- Morita, T., Kuribara, F., Shiozawa, Y., and Sugano, S. (2003). A novel mechanism design for gravity compensation in three dimensional space. In *Proceedings 2003 IEEE/ASME International Conference on Advanced Intelligent Mechatronics (AIM 2003)*, volume 1, pages 163–168. IEEE.
- Nakayama, T., Araki, Y., and Fujimoto, H. (2009). A new gravity compensation mechanism for lower limb rehabilitation. In *2009 International Conference on Mechatronics and Automation*, pages 943–948. IEEE.